Biological differences between FIM2 and FIM3 fimbriae of Bordetella pertussis: not just the serotype

Soraya Matczak, Valérie Bouchez, Pauline Leroux, Thibaut Douché, Nils Collinet, Annie Landier, Quentin Giai Gianetto, Sophie Guillot, Julia Chamot-Rooke, Milena Hasan, et al.

Journal Pre-proof

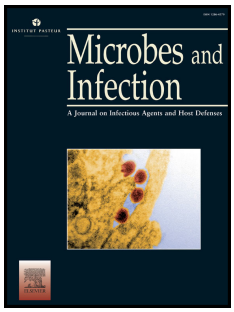

Biological differences between FIM2 and FIM3 fimbriae of *Bordetella pertussis*: not just the serotype

Soraya Matczak, Valérie Bouchez, Pauline Leroux, Thibaut Douché, Nils Collinet, Annie Landier, Quentin Giai Gianetto, Sophie Guillot, Julia Chamot-Rooke, Milena Hasan, Mariette Matondo, Sylvain Brisse, Julie Toubiana

PII: S1286-4579(23)00055-2

DOI: https://doi.org/10.1016/j.micinf.2023.105152

Reference: MICINF 105152

To appear in: *Microbes and Infection*

Received Date: 16 February 2023

Revised Date: 17 May 2023

Accepted Date: 19 May 2023

Please cite this article as: S. Matczak, V. Bouchez, P. Leroux, T. Douché, N. Collinet, A. Landier, Q.G. Gianetto, S. Guillot, J. Chamot-Rooke, M. Hasan, M. Matondo, S. Brisse, J. Toubiana, Biological differences between FIM2 and FIM3 fimbriae of *Bordetella pertussis*: not just the serotype, *Microbes and Infection*, https://doi.org/10.1016/j.micinf.2023.105152.

Biological differences between FIM2 and FIM3 fimbriae of *Bordetella pertussis*: not just the serotype

Soraya Matczak[a,#], Valérie Bouchez[a,b,#], Pauline Leroux[a], Thibaut Douché[c], Nils Collinet[a], Annie Landier[b], Quentin Giai Gianetto[c,d], Sophie Guillot[b], Julia Chamot-Rooke[c], Milena Hasan[e], Mariette Matondo[c], Sylvain Brisse[a,b,$], Julie Toubiana[a,b,f,$,*]

a Institut Pasteur, Université Paris Cité, Biodiversity and Epidemiology of Bacterial Pathogens, 28, rue du Docteur Roux, 75015 Paris, France.

b National Reference Center for Whooping Cough and other Bordetella infections, Institut Pasteur, 28, rue du Docteur Roux, 75015 Paris, France.

c Institut Pasteur, Université Paris Cité, CNRS UAR2024, Proteomics Platform, Mass Spectrometry for Biology Unit, 28, rue du Docteur Roux, 75015 Paris, France.

d Institut Pasteur, Université Paris Cité, Bioinformatics and Biostatistics Hub, 28, rue du Docteur Roux, 75015 Paris, France.

e Institut Pasteur, Université Paris Cité, Cytometry and Biomarkers Unit of Technology and Service (CB UTechS), 28, rue du Docteur Roux, 75015 Paris, France.

f Department of General Pediatrics and Pediatric Infectious Diseases, Hôpital Necker–Enfants Malades, APHP, Université Paris Cité, 149, rue de Sèvres, 75015 Paris, France.

# These authors contributed equally

$ These authors share senior co-authorship

***Corresponding author:** Julie Toubiana

Université Paris Cité, Institut Pasteur, Biodiversity and Epidemiology of Bacterial Pathogens, Paris, France.

28, rue du Docteur Roux, 75015 Paris, France, UE

Email: julie.toubiana@pasteur.fr

Tel: +33 (0)1 40 61 37 96

Fax: +33 (0)1 40 61 35 33

ORCID: 0000-0001-9561-669X

ABSTRACT

Introduction: *Bordetella pertussis* still circulates worldwide despite vaccination. Fimbriae are components of some acellular pertussis vaccines. Population fluctuations of *B. pertussis* fimbrial serotypes (FIM2 and FIM3) are observed, and *fim3* alleles (*fim3-1* [clade 1] and *fim3-2* [clade 2]) mark a major phylogenetic subdivision of *B. pertussis*.

Objectives: To compare microbiological characteristics and expressed protein profiles between fimbrial serotypes FIM2 and FIM3 and genomic clades.

Methods: A total of 23 isolates were selected. Absolute protein abundance of the main virulence factors, autoagglutination and biofilm formation, bacterial survival in whole blood, induced blood cell cytokine secretion, and global proteome profiles were assessed.

Results: Compared to FIM3, FIM2 isolates produced more fimbriae, less cellular pertussis toxin subunit 1 and more biofilm, but auto-agglutinated less. FIM2 isolates had a lower survival rate in cord blood, but induced higher levels of IL-4, IL-8 and IL-1β secretion. Global proteome comparisons uncovered 15 differentially produced proteins between FIM2 and FIM3 isolates, involved in adhesion and metabolism of metals. FIM3 isolates of clade 2 produced more FIM3 and more biofilm compared to clade 1.

Conclusion: FIM serotype and *fim3* clades are associated with proteomic and other biological differences, which may have implications on pathogenesis and epidemiological emergence.

Keywords: *Bordetella pertussis*; phylogenetic clade; serotype; fimbriae; proteomics; virulence

ABBREVIATIONS

AC-Hly: Adenylate Cyclase Haemolysin

aPV: acellular Pertussis Vaccines

BGA: Bordet-Gengou Agar

B. pertussis: *Bordetella pertussis*

CFU: Colony-Forming Unit

DIA-MS: Data Independent Acquisition Mass Spectrometry

FC: Fold-Change

FDR: False Discovery Rate

FHA: Filamentous Hemagglutinin

FIM: fimbriae

LOQ: Limit Of Quantification

MOI: Multiplicity Of Infection

OD: Optical Density

PRM: Parallel Reaction Monitoring

PRN: Pertactin

PT: Pertussis Toxin

S1-PT: Pertussis Toxin Subunit 1

SS: Stainer and Scholte

wPV: whole cell pertussis vaccines

1. Introduction

Whooping cough is a highly contagious respiratory disease whose main causative agent is the gram-negative bacterium *Bordetella pertussis* [1]. Despite the introduction of whole cell pertussis vaccines (wPV) in the late 1950s, and of acellular pertussis vaccines (aPV) in the mid 1990s in many high-income countries, pertussis strains are still circulating worldwide [2]. Among the documented evolutionary changes observed in contemporaneous *B. pertussis* populations, variation in the antigens contained in vaccines are of high concern given their potential negative impact on vaccine effectiveness [2, 3].

aPVs target 2 to 5 different *B. pertussis* antigens: pertussis toxin (PT), pertactin (PRN), filamentous hemagglutinin (FHA) and the two serologically distinct fimbriae FIM2 and FIM3. FIM2 or FIM3 major subunits have 60 % amino acid sequence identity between each other and these fimbriae contain the common minor tip subunit FIMD [4] but are characterized by different properties, as illustrated by different methods required for their purification [4]. *B. pertussis* typically express either FIM2 or FIM3, or much less commonly, both FIM2 and FIM3 [4]. The relative frequencies of serotypes FIM2 and FIM3 have fluctuated since the introduction of vaccination: whereas FIM2 serotype was predominant in unvaccinated populations [4], a shift towards FIM3 serotype occurred after the introduction of pertussis vaccines [5, 6]. More recently, a reverse trend of FIM2 reemergence is being observed in France (up to 27.9 %) and other European countries [6, 7].

The drivers of the population fluctuations of FIM serotypes remain unclear. At the molecular level, the expression of fimbriae is regulated both by the BvgA/S two component system and by the length of a homopolymeric tract located in the promoter sequence of genes *fim2* and *fim3* [4, 8]. At the population level, one possibility is that vaccine-induced immune pressure might drive evolutionary shifts in the type and level of expression of fimbriae; but as not all acellular pertussis vaccines contain fimbrial proteins[4, 9], recent shifts in serotype may be linked to

frequency-dependent selection [4, 9]. Another possibility is that variable biological properties between isolates of the two FIM serotypes would impact colonization, carriage, transmission, and immune escape of *B. pertussis* isolates [10]. In favor of the latter hypothesis, some studies described a role of fimbriae in strain agglutination and biofilm formation properties [11, 12], as well as in the regulation of initial inflammatory responses to pertussis infection [13].

B. pertussis populations are phylogenetically structured into clades that have emerged successively and are marked by key mutations in genes encoding aPV antigens, such as in the Ptx promotor (from *ptxP1* to *ptxP3*), the genes for subunit A of Ptx (from *ptxA2* to *ptxA1*), and pertactin (from *prn1* to *prn3* and *prn2*) [3]. An important landmark mutation is also observed in the *fim3* gene itself, which displays the two predominant alleles *fim3-1* and *fim3-2* [2, 3]. *B. pertussis* isolates of serotype FIM2 are mainly observed in the *fim3-1* clade (clade 1), while FIM3 isolates represent the vast majority of isolates of both *fim3-1* and *fim3-2* (clade 2). Whereas clade 1 is ancestral, clade 2 evolved in the 1980s (wPV period) and, in France, has subsequently increased rapidly in frequency (up to 42 %, observed in year 2019), especially during the aPV period [2, 3, 14]. Differential susceptibility to vaccine-induced immunity, or biological differences between *fim3-1* and *fim3-2* isolates in terms of disease severity and transmission, could be associated with this emergence [3]. However, phenotypic variation between clades 1 and 2 remains to be investigated.

To provide novel insights into the drivers of emergence of FIM serotypes and *fim3* clades of *B. pertussis*, we investigated the biological variation among them, including *in vitro* vaccine antigen expression, biofilm formation, autoagglutination, global proteomics, and immunological features.

2. Materials and methods

2.1 *Selection of B. pertussis isolates*

From a set of 1120 *B. pertussis* isolates with available genomic sequences in the National Reference Center (NRC) for Whooping Cough and other Bordetella infections, we selected for this study 19 isolates (e.g., Fig. S1**)**, all from infants under 6-month-old with whooping cough and collected between 2008 and 2019. Isolates had been serotyped to detect the production of fimbrial proteins FIM2 and FIM3 according standard recommendations [15]. The selection process is described in detail in the Supplementary appendix). Selected isolates (e.g., Table S1**)** corresponded to 8 FIM2 isolates and 11 FIM3 isolates. Among the 11 FIM3 isolates, 6 were from *fim3-1* (clade 1) and 5 were from *fim3-2* (clade 2, e.g., Table S1). All isolates of FIM2 serotype (n=8) were from clade 1 (given the absence of FIM2 isolates from clade 2), and their comparators were therefore the 5 FIM3 isolates that also belonged to clade 1. One isolate (CIP1672), which does not produce FHA (a protein involved in auto-aggregation properties), and 3 additional isolates without fimbriae production (FIM-, from clade 1) were also used in auto-agglutination and biofilm assays.

2.2 *Culture conditions*

B. pertussis isolates were grown at 36 +/- 1 °C for 72 h on Bordet-Gengou Agar plates (BGA) and further grown in bacterial layer on BGA for 24 h [15]. Bacterial suspensions were prepared in the synthetic Stainer and Scholte (SS) liquid medium [16] and calibrated to an optical density (measured at 650 nm) value of 1 +/- 0.1 (OD_{650}-1). This standardized OD650-1 suspension was i) immediately used for biological assays (auto-agglutination and biofilm assays) or, ii) 1/10 diluted in a new SS medium and cultured at 36°C with 100 RPM agitation; the culture was

stopped at a final OD650- 1 +/- 0.1 and this suspension was used for cord blood infection or for proteomic analyses. At each stage, the absence of BGA contamination was visually controlled.

2.3 *Auto-agglutination tests*

For each isolate, 4 ml of the calibrated OD_{650}-1 bacterial suspension prepared in SS medium were incubated in static condition at room temperature for 4 hours. Every hour (H0, H1, H2, H3, H4), the OD_{650} of the top fraction of the suspension was measured [17]. Auto-agglutination index was calculated as follows: (OD_{650} initial-Ho – OD_{650} final-H4)*100. In each experiment, one control isolate that does not produce FHA (CIP1672) and which is known to have very low agglutination properties, was used [18].

2.4 *Microplate biofilm assays*

For each isolate, the calibrated bacterial suspension OD_{650}-1 prepared in SS medium was ¼ diluted and 200 µL of this dilution were added in triplicate in 96-well plate. For each experiment, negative controls (SS medium) were added. The plates were incubated at 37°C for 24 h and 48 h, and then washed with water to eliminate planktonic bacteria. Bacteria on the well surface were stained with 200 µL of Crystal Violet 0.1 %/well (Sigma Aldrich, V5265 1 %) for 30 minutes [17]. Plates were washed with water and dried, Crystal Violet was then solubilized with ethanol 95 % and OD_{595} was measured [17]. For each isolate, biofilm formation was assessed by the mean OD values obtained for the triplicates. OD values for each experiment were corrected by subtracting the values deriving from the negative controls.

2.5 *Whole blood ex vivo* infection and *B. pertussis survival*

Fresh heparinized cord blood instead of whole blood from adult donor was used to mimic an infection in early infancy. Cord blood samples were provided by the biocollection of the Cell

Therapy Unit from the Biological Resources Center of Saint-Louis Hospital (Paris, France). 200 µL of whole cord blood was added to each well of a flat bottom 48-well plates and incubated with 200 µL of bacterial suspension diluted in RPMI medium (RPMI Medium 1640 (1X) + GlutaMAXTM-I, Gibco) to the desired concentration, to reach a Multiplicity of infection (MOI, ratio bacteria/cell) of approximately 10. The plates were then incubated at 37°C and 5% CO2 for 4 h (for bacterial survival assays) or 22 h (for cytokine assays). For survival assays, after 4 h of whole cord blood infection, 50 µl of the suspension were serial diluted and plated on BGA to estimate *B. pertussis* survival. Survival was expressed as a percentage of the initial *B. pertussis* load. Anti-PT IgG antibody concentrations were measured in all cord blood samples (they were originated from 9 different donors) used in this study (kit Savyon SeroPertussis^{TM} Toxin IgG 1231-01D); all of them had IgG titers < 40 UI/ml and were therefore considered seronegative.

2.6 *Cytokine measurements*

After 22 h of whole cord blood cells incubation with *B. pertussis*, the plates were centrifuged at 4 °C (1500 rpm) and 150 µl of serum was collected, aliquoted and then stored at -20 °C. Then 19 analytes (cytokines, chemokines, growth factor and adhesins) were measured in the sera (e.g., Table S2), using the Human Magnetic Luminex Assay 20 Plex kit (R&D systems, LXSAHM-20) and the Bioplex 200 technology according to the manufacturer's recommendations. Data analyses are detailed in the Supplementary appendix.

2.7 *Measurement of cellular protein expression by two complementary MS proteomic approaches*

For each strain, 1 ml of standardized OD_{650}-1 suspension was transferred in an Eppendorf tube and centrifuged during 10 min at 4 °C and at 8000 rpm. The pellet was suspended in 100 µl of

a Urea Buffer 8M/Tris HCl 0.1M lysis buffer and then sonicated during 5 cycles of 30 seconds and frozen at -80 °C before use for proteomic characterization.

PRM (Parallel Reaction Monitoring) is a proteomic method [19, 20], allowing the absolute quantification of targeted proteins. In PRM a set of unique peptides are used as surrogates and specifically targeted. The method is based on the identification/quantification of endogenous peptides related to their isotopically-labeled counterparts used as standards and spiked into each sample. Here, we targeted the 6 main virulence factors produced by *B. pertussis* (PT, FHA, PRN, FIM2 and FIM3, AC-Hly) all of which except AC-Hly are included in acellular vaccines. Proteins quantities were expressed in nanograms.

We then used a large-scale proteome analysis based on Data Independent Acquisition Mass Spectrometry (DIA-MS) [21]. DIA-MS mode consists in consecutive precursor isolation windows which are fragmented to obtain complex product ion spectra used to match with a *Bordetella* reference spectral library that we constituted considering the proteomes of *B. pertussis* strains Tohama I (Uniprot: UP000002676) and B1917 (Uniprot: UP000031744). All details regarding proteomic methods used are found in the Supplementary appendix.

2.8 *Data processing and statistical analyses*

For each isolate, levels of proteins quantified by PRM, and OD values from biofilm, auto-agglutination and survival assays were expressed in median and interquartile range. All graphs and figures were obtained with GraphPad Prism 8.4.3. Dot blots differences between groups of isolates (isolates of FIM2 vs. FIM3 serotypes, and from clade 1 vs. clade 2) were identified with nonparametric Mann Whitney U test or Kruskal-Wallis tests followed by post-hoc multiple comparisons Dunn’s test, when appropriate.

Cytokine heatmaps were made and analyzed with Qlucore OMICS explorer 3.7 (version 1.1.463), and cytokine dot plots with GraphPad Prism 8.4.3. A p-value < 0.05, or an adjusted p-value value for Luminex assays < 0.05 was considered statistically significant.

For DIA-MS, data from three biological samples for each condition (replicates) were analyzed and compared between groups of isolates. When comparing two biological conditions, proteins exhibiting less than six quantified values in at least one biological condition were discarded from the list to ensure a minimum of replicability. Next, proteins without any value in one or the other biological condition have been considered as proteins quantitatively present in a condition and absent in another. They have therefore been set aside and considered as differentially abundant proteins. After log2 transformation of the intensities of the leftover proteins, missing values were imputed using the "impute.mle" function of the R package imp4p [22]. Proteins with a fold-change (FC) under 2 (i.e. absolute log2(FC)<1) have been considered not significantly differentially abundant. Statistical testing of the remaining proteins (having a fold-change over 2) was conducted using a limma t-test thanks to the R package limma [23]. An adaptive Benjamini–Hochberg procedure was applied on the resulting p values thanks to the function "adjust.p" of R package cp4p [24], using the 'slim' method to estimate the proportion of true null hypotheses among the set of statistical tests [25]. The proteins associated to an adjusted p-value inferior to a false discovery rate (FDR) of 1% have been considered as significantly differentially abundant proteins. Finally, the proteins of interest are therefore those which emerge from this statistical analysis supplemented by those which are absent from one condition and present in another. Results of these differential analyses are summarized in volcano plots and heatmaps. Heatmaps display the mean z-scores of proteins with small p-values along the biological samples. A z-score is a log2(intensity) value minus the average divided by the standard deviation of the log2(intensity) values of a protein in all the samples. A mean z-score have been computed from z-scores of the 3 replicates of a same biological sample.

Hierarchical clustering on the left side of heatmaps are estimated from the mean z-scores using a Pearson correlation-based distance and the Ward's method.

3. Results

3.1 *FIM2 isolates produce more fimbriae and less cellular S1-PT than FIM3 isolates*

To investigate whether the cellular abundance of key virulence factors (S1-PT, FHA, PRN and AC-Hly) was variable according to the FIM serotype, we quantified their absolute levels as well as the major subunits of fimbriae FIM2 and FIM3, using a targeted proteomics approach by PRM (e.g., Table S3). For this, 6 FIM3 and 8 FIM2 isolates (total n=14, all genotyped as *ptxP3, fim3-1*) were used (e.g., Fig. S1). All isolates presented a similar median generation time (hence growth rate) in SS medium: 7.04 hours for FIM3 and 7.46 hours for FIM2 isolates (p=0.23, e.g., Fig. S2), even though we noticed a higher dispersion for FIM2 isolates, with generation times ranging from 5.65 to 8.15 hours.

As expected, FIM2 and FIM3 isolates produced almost exclusively FIM2 and FIM3, respectively. When compared to FIM3 isolates, median levels of fimbriae produced by FIM2 isolates were much higher (2.80 ng of FIM2 vs. 0.75 ng of FIM3, p=0.0012, e.g., Fig. S3**)**, whereas the median levels of S1-PT produced by FIM2 isolates were lower (1.30 ng vs. 2.10 ng, p=0.004) (e.g., Fig. 1**)**. No significant difference in levels of the three other tested virulence factors (FHA, PRN and AC-Hly) was observed (e.g., Fig. 1). Of note, a residual production of FIM2 was observed in FIM3 isolates, as well as FIM3 in FIM2 isolates ($<10^{-11}$ng) as already reported [8].

3.2 *FIM2 isolates are characterized by a lower auto-agglutination and a higher biofilm formation compared to FIM3 isolates*

As *B. pertussis* can adapt to its environment through a higher persistence via agglutination or

biofilm formation [26], we evaluated these properties on the same 14 isolates. Three FIM deficient (FIM-) isolates were used as controls. At 4 hours of incubation, we observed a much lower auto-agglutination in FIM2 isolates compared to the FIM3 ones, with a median Auto-Agglutination Index (IAA) of 7.00 vs. 91.67, respectively (p=0.002; e.g., Fig. 2A**)**. A significant IAA difference between FIM2 and FIM3 isolates was already observed as of H2 (IAA-H2 of 2.71 vs 89.11, p=0.002, data not shown). The IAA of FIM2 isolates was comparable to control (FHA-) isolates (p > 0.99). Measurement of biofilm formation by Crystal Violet revealed that FIM2 isolates produced more biofilm than FIM3 isolates, with a median OD595nm at 24 hours of 1.11 vs. 0.35 (p=0.007), and at 48 hours 2.30 vs. 0.79 (p=0.01), respectively **(**e.g., Fig. 2A and 2C). The 3 FIM- isolates had comparable auto-agglutination and biofilm formation properties as the FIM3 ones (e.g., Fig. 2A-C**).**

3.3 *FIM2 isolates induce a distinct cytokine release profile, when compared to FIM3 isolates*

To analyze bacterial resistance to whole blood bactericidal activity and immunological ex vivo processes induced by *B. pertussis* according to serotype, we used human cord blood, considered to reflect the neonatal conditions. The survival rate was lower for FIM2 isolates than for FIM3 isolates (median survival rate: 3.62 % vs. 22.00 %, respectively, p=0.04; e.g., Fig. 2D).

Levels of cytokines and chemokines were also measured in sera following ex vivo cord blood infection by using FIM2 or FIM3 isolates (Fig. 3). After infection, levels of inflammatory markers were elevated for 16/19 measured proteins (adjusted p-value=0.049) as compared to non-infected cord blood (e.g., Fig. S4**)**. Among these 16 markers, we observed markedly higher levels of IL-4 and higher levels of IL-8 and IL-1β and almost no IL-2 secretion and lower levels of IL-6 following infection with FIM2 isolates, when compared with FIM3 isolates (adjusted p-value=0.049, e.g., Fig. 3).

301

302 3.4 *Isolates from clade 2 produce more FIM3 and more biofilm*

303 To investigate biological differences between *B. pertussis* genomic clades, we selected 11 FIM3
304 isolates: 6 from clade 1 and 5 from clade 2 (n=11). These isolates presented a similar median
305 generation time (hence growth rate) in SS medium: 7.04 hours and 6.86 hours for isolates from
306 clade 1 and 2, respectively (p=0.43, e.g., Fig. S2). Absolute quantification of proteins by PRM
307 revealed that isolates from clade 2 expressed more FIM3 than those from clade 1 (median levels
308 of FIM3: 1.06 ng vs. 0.59 ng, respectively, p=0.004, e.g., Fig. 4). No difference in protein
309 abundance of other tested proteins (S1-PT, FHA, PRN and AC-Hly) was observed between
310 isolates from clade 1 and 2 (e.g., Fig. 4). Auto-agglutination properties were similar between
311 isolates from clade 1 and 2 (p=0.19, e.g., Fig. 5A**)**. Levels of biofilm production were higher in
312 clade 2 than in clade 1 isolates after 24 hours of incubation (median OD595nm at 0.86 vs. 0.35,
313 respectively, p=0.011; e.g., Fig. 5B), but this did not reach significance at 48 hours (p=0.14,
314 e.g., Fig. 5C).
315 We also proceeded to an in vitro cord blood infection by 4 FIM3 *B. pertussis* isolates (2 from
316 clade 1 and 2 from clade 2). A difference in terms of survival was observed between clades but
317 without reaching significance (median survival rates: 3.40 % vs. 22.0 % vs. for clades 2 and 1,
318 respectively, p=0.09, e.g., Fig. 5D). Levels of cytokines and chemokines were also measured
319 in sera following in vitro cord blood infection. As previously observed, levels of inflammatory
320 markers were overall elevated, with 14/19 measured proteins significantly elevated compared
321 to non-infected cord blood (adjusted p-value<0.05, e.g., Fig. S5). However, no significant
322 difference was observed between isolates from genomic clades 1 and 2.

323

324 3.5 *Large-scale proteome analysis of B. pertussis circulating isolates*

To test whether the abundance of *B. pertussis* proteins, beyond the main virulence factors, could vary according to serotype (FIM2 vs FIM3) and to genomic clade (clade 2 vs clade 1), we performed a large-scale proteomics analysis using DIA-MS to obtain a comprehensive view of the proteome [21, 27]. In all samples, we detected a total of 2,482 different proteins (Table S4). The median number of proteins detected per isolate was 2,407 (ranging from 2,298 to 2,440, which represents 64.6 to 68.6% of the entire *B. pertussis* proteome that contains a median value of 3,555 encoded proteins [28]. 2,111 proteins (85.05%) were detected in all the samples (in all the 3 replicates of all the strains) with similar distribution of intensities suggesting relatively consistent quantification of proteins. Based on the pre-defined stringent selection criteria (|log2(FC)|>1, p-value<1%), 15 proteins were found differentially abundant when comparing FIM2 and FIM3 isolates. In addition, one protein, the replication-associated recombination protein A (WP_003814028.1), was only detected in FIM2 isolates. Of note, 26.7 % of proteins represented in Fig 6B were known to be bvg-regulated [29]. Among the 15 differentially expressed proteins, 12 were more abundant in FIM2 isolates, among which FIM2, a molybdenum transport system permease ModC (Q7VUJ4), a ferredoxin (Q7VS61), a putative zinc-binding dehydrogenase (Q7VT48) and the ferric siderophore receptor BfrC (Q7VT87) (e.g., Fig 6., Table S5). The three less abundant proteins in FIM2 isolates were a putative exported protein (Q7VUI9), a urease accessory protein UreD (P0A4R4), and a ribosomal subunit interface protein (WP_019247685.1). We did not observe a differential expression among proteins involved in *B. pertussis* biofilm formation [30, 31]. Of note, the *Bordetella* intermediate protein A BipA (Q7VZ27), involved in *B. pertussis* colonization and biofilm formation [30], tended to be slightly more abundant in FIM2 than in FIM3 isolates (|log2(FC)|=0.68 ; p-value=0.09, e.g., Table S5). Concerning proteins represented in Figure 6B, we found interactions among some of them using STRING interaction network (https://string-db.org/) [32]. Proteins of these networks could be associated with virulence patterns.

A first network grouped some proteins encoded by genes localized within the "*his"* operon, and involved in histidine biosynthesis (Q7VZ1,2,3 &4 and Q7VSY6,8 &9). Histidine biosynthesis and transport genes can be regulated by a variety of mechanisms including a repressor protein and various RNA structures, such as transcriptional attenuators and T-box riboswitches [33]. Observed variations in histidine biosynthesis could affect bacterial fitness. A second network included genes of 2 proteins (Q79GQ2 &5) from T3SS named Bcr4 and BcrH1 and a third one contained 2 proteins (Q7VT48 &50), one of them being a putative zinc binding deshydrogenase. Not all the proteins from *his* or *T3SS* operons were found differentially expressed in our proteomic analysis: some were not detected, and some were just below significance. For all these proteins related either to T3SS or to iron metabolism, metal transport metabolic pathways can be connected as expression of type III secretion system can be affected by several factors such as iron starvation, which leads to an upregulation of T3SS genes in the ancestral species *B. bronchiseptica* [34]. Targeted transcriptomic and proteomic analyses focused on all the proteins contained in these operons could help solving this issue.

When comparing FIM3 isolates from clades 1 and 2, 22 proteins were differentially produced (|log2(FC)|>1, p-value<0.1 %), e.g., Fig. S6, Table S6). Of note, 27.3% of proteins represented in Fig S6B were known to be bvg-regulated according to Moon et al [29]. Among them, 12 proteins were more abundant in isolates from clade 2, including FIM3 (as P17835 and as WP_019248658.1; e.g., Table S6). We also identified the ferric siderophore receptor BfrC (Q7VT87), a putative zinc-binding dehydrogenase (Q7VT48), a putative membrane protein (Q7VYP6) and a putative cold shock-like protein (Q7VSQ7). Ten proteins were less abundant in clade 2 isolates (e.g., Fig. S6), including a multidrug resistance protein NorM (Q7VYS9), a putative exported protein (Q7VUI9), a putative inner membrane efflux protein (Q7VWD9), a putative 2-hydroxyacid dehydrogenase (Q7VU57), and two proteins involved in T3SS (proteins Q79GQ1 and Q7VWI3). We did not observe between clades a differential expression of

proteins involved in *B. pertussis* biofilm formation [30, 31]. However, BipA (Q7VZ27) was slightly more abundant in clade 2 than clade 1 isolates (|log2(FC)|=0.42; p-value=0.09). FIM2 was also detected in isolates from the two clades without significant difference.

4. Discussion

Here, we analyzed the abundance of major virulence factors, whole cell proteomes, and other biological differences, of *B. pertussis*. We used a combination of two highly innovative proteomic approaches, PRM and DIA-MS. Previous proteomic studies on *B. pertussis* used rather gel-based proteomics approaches [35, 36]. Whereas the most recent proteomics studies based on mass spectrometry obtained 20 to 30% coverage of *B. pertussis* theorical proteome [37, 38], we reached more than 60% coverage highlighting the power of our technology to analyze bacterial proteomes. Such high coverage was reported in previous DIA analysis of the *E. Coli* proteome [39]. Furthermore, the previous studies on *B. pertussis* proteome aimed to compare recently circulating isolates to historical ones, or recent isolates according to PRN expression status and *ptxP* and *fhaB* alleles [37, 40-42], whereas here we compared expression levels of vaccine antigens as well as whole proteome according to FIM serotype and *fim3* clade, using a large set of isolates. Our study design enables us to address the association of these variations with precise phenotypic features, enabling the formulation of specific hypotheses on the impact of recent molecular changes.

4.1 *Differences in fimbriae production and its association with biofilm formation*

The recent increase of FIM2 serotype observed in some European countries [6, 7], raised the question of possible differences between serotypes at the global proteome level and their implications on specific biological properties. The variations of FIM2 and FIM3 production we observed for each isolate were assessed from five highly reproducible biological replicates, indicating that possible heterogeneities among individual cells within cultures were negligible.

Here, we found that one prominent difference between FIM serotypes was the higher production of fimbriae by FIM2 isolates. This result confirms but also quantifies, previous findings observed with electron microscopy [4, 43]. In addition, our phenotypic experiments showed that FIM2 isolates produced more biofilm, suggesting a correlation between levels of fimbriae and biofilm formation. This correlation has already been observed in other pathogens [44], but a direct causality still needed to be investigated in *B. pertussis*. Here, the observed variations in biofilm formation could also be due to proteins other than fimbriae that are differentially produced or organized at the cell surface in isolates of different FIM serotype; Our whole proteome analyses showed slightly higher levels of BipA proteins in FIM2 isolates compared to FIM3 ones. BipA, an intermediate phase protein, was described as the most abundant surface-exposed protein in *B. pertussis* biofilms [30] and reported to prevent auto-agglutination and to promote biofilm formation by *B. holmesii* isolates [45]. BipA could therefore explain the variable auto-agglutination and biofilm formation properties of FIM2 and FIM3 isolates. Interestingly, we also observed that FIM3 isolates from the recently emerged clade 2 also produces more fimbriae than those from clade 1; this property of clade 2 is also associated with more biofilm formation and a tendency for higher BipA production. Further investigations are needed to determine whether the difference in biofilm formation is a consequence of the expression levels of fimbriae or an indirect effect of other proteins such as BipA. Overall, this work puts forwards the hypothesis that the drivers of emergence of both FIM2 and clade 2 may be linked to adhesion and biofilm properties.

In our study, we observed a much lower auto-agglutination of FIM2 isolates compared to FIM3 ones. FHA is the main protein involved in auto-agglutination in *B. pertussis* [46]. Protein quantification by PRM revealed that all tested *B. pertussis* isolates produce similar amounts of FHA. Fimbriae proteins are also known to be involved in autoagglutination of *B. pertussis* [12], with a higher autoagglutination observed in strains producing high FIM3 levels. This suggests

that either the nature of serotype 2 fimbriae, or their high expression levels at the bacterial surface, may interfere with FHA agglutination properties. Cooperation between fimbriae and FHA for adhesion and immune modulation has been suggested in *B. bronchiseptica* [47]. The FIMD adhesin might also be of importance in these possible interactions, as its involvement on human cells adhesion has been demonstrated [48]. We did not identify any difference in FIMD production between FIM2 and FIM3 isolates by the DIA proteomic approach, however future studies are needed to explore cell surface conformational modifications associated with FIM production levels and their potential impact on bacteria-bacteria adhesion rather than on human cell adhesion.

4.2 *Differences in other vaccine antigens production*

Concurrently with the change in FIM serotype, the recent emergence of isolates that do not produce PRN (PRN-) has been reported in many countries with high acellular vaccine coverage (e.g., in France since 2007 to 2019 from 5.6 to 52.1%) [6, 49]. To avoid interference with this effect, our study only included isolates that produce PRN, and we did not observe any difference in terms of PRN levels between isolates from FIM2 and FIM3 serotypes. This suggests a similar vaccine-driven selective pressure for PRN loss on all *B. pertussis* isolates, regardless of FIM serotype. Indeed, although PRN deficiency was first observed in FIM3 isolates, more recently this was also identified within FIM2 isolates, in Spain [50] and Slovenia [51].

Our PRM analysis showed that FIM2 isolates display lower levels of cellular-associated fraction of S1-PT, when compared with FIM3 isolates. This is a potentially important observation raising the possibility of a differential virulence of FIM2 isolates. The *ptx* and *ptl* genes, encoding PT subunits S1-S5 and PT secretion system respectively, are co-transcribed under the control of the *B. pertussis ptx* promoter (*ptx*P*)* [52]. At the genomic level, *ptx-ptl* locus and *fim* encoding genes are not related. Here, FIM2 and FIM3 isolates are both

449 characterized by a *ptxP3*-type promoter, excluding variations of *ptxP* as an explanatory factor.
450 In a landmark work, Mooi et al. have suggested that *ptxP3* emerging lineages produced more
451 PT than ancestral *ptxP1* ones [53]. However, other teams suggested that *ptxP3* is not an up-
452 promoter and therefore should not affect PT expression (Stibitz S., International Bordetella Lab
453 Meeting 2021. "unpublished"). Here, we note that the FIM serotypes of the 8 isolates used by
454 Mooi et al. (also controlled by the French NRC for Bordetella infections) were not
455 homogeneous: 2 *ptxP1* isolates produced FIM2. Hence, the Mooi et al. *ptxP1-ptxP3* comparison
456 may have been affected in part by the fimbriae serotype of isolates, rather than solely by the
457 *ptxP1-ptxP3* genotypes. Further investigations of isogenic mutants are needed to determine
458 whether fimbriae proteins can interfere with levels of intracellular PT, and whether similar
459 findings are observed at the transcriptome and secretome levels.

460

461 4.3 *Differences in cytokine profiles in whole cord blood induced by B. pertussis isolates*

462 In our study, we showed that FIM2 isolates had lower survival rate in blood and induced higher
463 secretion of IL-4, IL-8 and IL-1β than FIM3 isolates. Since infants of less than 3-months are
464 the most vulnerable population to pertussis, using this experimental *in vitro* setup [54], which
465 reflects the response immune signatures of young infants, was considered to be relevant [55].
466 IL-4 is involved in the regulation of inflammation and Th2 response [56], IL-8 induces
467 chemotaxis in target cells and stimulates phagocytosis [57] and IL-1β is a potent pro-
468 inflammatory cytokine that is crucial for host-defense responses to infection [58]. Conversely,
469 FIM3 isolates were associated with more IL-2 and IL-6 secretion; IL-2 is involved in T-cell and
470 Th1 response [59] and IL-6 is a key pro-inflammatory cytokine associated to the stimulation of
471 acute phase proteins [60]. Interestingly, natural infection and immunization with wPVs both
472 induce a pattern of Th1/Th17 response, while aPVs induce a Th2 response [61, 62], similarly

to our in vitro results on whole blood stimulation with FIM2 isolates. The differences found here between FIM2 and FIM3 induction are remarkable and suggest a distinct immune reaction profile depending on *B. pertussis* serotype. FIM2 and FIM3 have been copurified and integrated jointly in fimbriae-containing aPVs. It has been shown that FIM2 is more immunogenic than FIM3 [4, 63, 64], in terms of antibody responses which is mostly Th2-dependent [61-63]. Our findings might be of importance in vaccine development, which needs to clearly identify the respective role of FIM2 and FIM3 on induction or modulation of immune responses. Interestingly, Kroes et al. suggested mild immunological activation of human airway epithelium by 3 different *B. pertussis* strains from unknown serotype, associated with the secretion of IL-6, CXCL8/IL-8 and the enrichment of genes involved in bacterial recognition and innate immune processes [65]. Our results suggest that these previously published results should be interpreted with regard to the serotype of the isolates that were studied. Further investigations are needed to make a link between these observations especially because they are using different study models (whole blood and epithelium).

4.4 *Differences in proteome profiles*

Most of *B. pertussis* virulence factors are regulated by the master two-component bvgAS system [29]. In our dataset, less than 30% of differential proteins were known as bvg-regulated. Most of the differential proteins identified with our large-scale proteome analysis of *B. pertussis* circulating isolates were related to transport of metal chemicals such as molybdenum, iron or zinc. Molybdenum has been described in other bacterial species such as *Pseudomonas aeruginosa*, to participate in anaerobic respiration, virulence, biofilm formation or intracellular survival within macrophages [66]. The higher levels of molybdenum transport system permease ModC (Q7VUJ4) in FIM2 isolates may be related to a greater biofilm production with FIM2 isolates [67]. Ferric siderophore receptor bfrC (Q7VT87) and ferredoxin (Q7VS61) were also more abundant in FIM2 isolates; as iron is crucial for *Bordetella* adaptation to nutrient

limitation [68], this finding suggests that FIM2 isolates may be more efficient at acquiring iron, which may have an impact on bacterial growth, fitness and survival. In our experiments, we used SS medium that contains iron as ferrous sulfate, which might have impacted our data; additional experiments on iron-restricted SS medium would be necessary to further investigate differential iron-regulated protein expression by FIM2 or FIM3 *B. pertussis* isolates. The proteins found more abundant in clade 2 also include iron or zinc related proteins, providing interesting hypotheses as to the evolutionary success of clade 2 and the impact of metal metabolism in *B. pertussis* evolution: there were some interesting commonalities between the phenotypic novelties observed in the two emerging groups FIM2 and *fim3-2* from their ancestors, in particular the increase in the expression of certain proteins such as FIM, iron or zinc metabolism proteins. This suggests that similar selective pressures are acting, leading to parallel evolution in emerging *B. pertussis* populations. Whereas the role of aPV vaccines that contain FIM proteins may drive the evolution towards higher levels of FIM expression, iron metabolism evolution might be driven by host adaptation, which is still recent for *B. pertussis* [3].

In conclusion, our study suggests that ongoing evolutionary shifts of *B. pertussis* towards expression of FIM2 rather than FIM3, and through emergence of clade 2, are associated with higher FIM fimbriae production and biofilm formation, potential immune escape, and differential metal metabolism. Furthermore, the lower cellular levels of PT in FIM2 isolates may impact *B. pertussis* virulence. These evolutionary observations raise important hypotheses that await experimental demonstration using FIM isogenic mutants to define the mechanisms behind these important phenotypic differences.

Authors' contributions

JT and SB conceived the study, and JT, VB, SM, MM and SB designed the study. SM, PL, NC, AL and SG collected the data, and SM, PL, NC, VB and JT were responsible for data management and analysis. SM, PL, MH were involved in cytokines data analysis. TD, QGG, JCR and MM were responsible for proteomic management and analyses. TD and QGG did the bioinformatic and statistical analyses. SM, VB and JT wrote the first draft of the manuscript, had access to and verified the source data, and were responsible for the decision to submit the manuscript. All authors drafted the manuscript for important intellectual content, contributed to the revision of the final version of the manuscript, and approved the final version submitted. All authors had full access to all the data in the study and had final responsibility for the decision to submit for publication.

Funding:

JT received funding from Ville de Paris as part of the EMERGENCE program. SM received funding from la Fondation pour la Recherche Médicale (FRM). SB received funding from INCEPTION program (ANR-16-CONV-0005).

Conflict of interest:

The authors declare no conflict of interest

Ethical approval:

This study was approved by the Comité Ethique et Scientifique pour les Recherches, les Etudes et les Evaluations dans le domaine de la Santé (CESREES, ethics and scientific committee for research, Studies and evaluation in health, registration number 2428977b, 11/02/2021) and authorized by the Commission Nationale de l'Informatique et des Libertés (CNIL, French data protection authority, registration number DR-2021-216, 20/07/2021).

548 **References**

549 [1] Carbonetti NH. Bordetella pertussis: new concepts in pathogenesis and treatment. Curr Opin
550 Infect Dis 2016;29:287-94.
551 [2] Lefrancq N, Bouchez V, Fernandes N, Barkoff AM, Bosch T, Dalby T, et al. Global spatial
552 dynamics and vaccine-induced fitness changes of Bordetella pertussis. Sci Transl Med
553 2022;14:eabn3253.
554 [3] Bart MJ, Harris SR, Advani A, Arakawa Y, Bottero D, Bouchez V, et al. Global population
555 structure and evolution of Bordetella pertussis and their relationship with vaccination. mBio
556 2014;5:e01074.
557 [4] Gorringe AR, Vaughan TE. Bordetella pertussis fimbriae (Fim): relevance for vaccines.
558 Expert Rev Vaccines 2014;13:1205-14.
559 [5] Caro V, Elomaa A, Brun D, Mertsola J, He Q, Guiso N. Bordetella pertussis, Finland and
560 France. Emerg Infect Dis 2006;12:987-9.
561 [6] Bouchez V, Guillot S, Landier A, Armatys N, Matczak S, Toubiana J, et al. Evolution of
562 Bordetella pertussis over a 23-year period in France, 1996 to 2018. Euro Surveill 2021;26.
563 [7] Mir-Cros A, Moreno-Mingorance A, Martin-Gomez MT, Codina G, Cornejo-Sanchez T,
564 Rajadell M, et al. Population dynamics and antigenic drift of Bordetella pertussis following
565 whole cell vaccine replacement, Barcelona, Spain, 1986-2015. Emerg Microbes Infect
566 2019;8:1711-20.
567 [8] Vaughan TE, Pratt CB, Sealey K, Preston A, Fry NK, Gorringe AR. Plasticity of fimbrial
568 genotype and serotype within populations of Bordetella pertussis: analysis by paired flow
569 cytometry and genome sequencing. Microbiology (Reading) 2014;160:2030-44.
570 [9] Azarian T, Martinez PP, Arnold BJ, Qiu X, Grant LR, Corander J, et al. Frequency-
571 dependent selection can forecast evolution in Streptococcus pneumoniae. PLoS Biol
572 2020;18:e3000878.

573 [10] Rodríguez ME, Hellwig SM, Pérez Vidakovics ML, Berbers GA, van de Winkel JG.
574 Bordetella pertussis attachment to respiratory epithelial cells can be impaired by fimbriae-
575 specific antibodies. FEMS Immunol Med Microbiol 2006;46:39-47.
576 [11] Irie Y, Mattoo S, Yuk MH. The Bvg virulence control system regulates biofilm formation
577 in Bordetella bronchiseptica. J Bacteriol 2004;186:5692-8.
578 [12] Otsuka N, Koide K, Goto M, Kamachi K, Kenri T. Fim3-dependent autoagglutination of
579 Bordetella pertussis. Sci Rep 2023;13:7629.
580 [13] Vandebriel RJ, Hellwig SM, Vermeulen JP, Hoekman JH, Dormans JA, Roholl PJ, et al.
581 Association of Bordetella pertussis with host immune cells in the mouse lung. Microb Pathog
582 2003;35:19-29.
583 [14] Centre National de Référence de la coqueluche et autres bordetelloses. Rapport annuel
584 d'activité 2019-2020. 2021.
585 [15] Guiso N, von Konig CH, Becker C, Hallander H. Fimbrial typing of Bordetello pertussis
586 isolates: agglutination with polyclonal and monoclonal antisera. J Clin Microbiol
587 2001;39:1684-5.
588 [16] Stainer DW, Scholte MJ. A simple chemically defined medium for the production of phase
589 I Bordetella pertussis. J Gen Microbiol 1970;63:211-20.
590 [17] Cattelan N, Jennings-Gee J, Dubey P, Yantorno OM, Deora R. Hyperbiofilm Formation
591 by Bordetella pertussis Strains Correlates with Enhanced Virulence Traits. Infect Immun
592 2017;85.
593 [18] Colombi D, Oliveira ML, Campos IB, Monedero V, Pérez-Martinez G, Ho PL.
594 Haemagglutination induced by Bordetella pertussis filamentous haemagglutinin adhesin (FHA)
595 is inhibited by antibodies produced against FHA(430-873) fragment expressed in Lactobacillus
596 casei. Curr Microbiol 2006;53:462-6.

[19] Kuzyk MA, Parker CE, Domanski D, Borchers CH. Development of MRM-based assays for the absolute quantitation of plasma proteins. Methods Mol Biol 2013;1023:53-82.

[20] Rauniyar N. Parallel Reaction Monitoring: A Targeted Experiment Performed Using High Resolution and High Mass Accuracy Mass Spectrometry. Int J Mol Sci 2015;16:28566-81.

[21] Ludwig C, Gillet L, Rosenberger G, Amon S, Collins BC, Aebersold R. Data-independent acquisition-based SWATH-MS for quantitative proteomics: a tutorial. Mol Syst Biol 2018;14:e8126.

[22] Giai Gianetto Q, Wieczorek S, Couté Y, Burger T. A peptide-level multiple imputation strategy accounting for the different natures of missing values in proteomics data. bioRxiv 2020.

[23] Ritchie ME, Phipson B, Wu D, Hu Y, Law CW, Shi W, et al. limma powers differential expression analyses for RNA-sequencing and microarray studies. Nucleic Acids Res 2015;43:e47.

[24] Giai Gianetto Q, Combes F, Ramus C, Bruley C, Couté Y, Burger T. Calibration plot for proteomics: A graphical tool to visually check the assumptions underlying FDR control in quantitative experiments. Proteomics 2016;16:29-32.

[25] Wang HQ, Tuominen LK, Tsai CJ. SLIM: a sliding linear model for estimating the proportion of true null hypotheses in datasets with dependence structures. Bioinformatics 2011;27:225-31.

[26] Cattelan N, Dubey P, Arnal L, Yantorno OM, Deora R. Bordetella biofilms: a lifestyle leading to persistent infections. Pathog Dis 2016;74:ftv108.

[27] Rauniyar N, Peng G, Lam TT, Zhao H, Mor G, Williams KR. Data-Independent Acquisition and Parallel Reaction Monitoring Mass Spectrometry Identification of Serum Biomarkers for Ovarian Cancer. Biomark Insights 2017;12:1177271917710948.

[28] NCBI. https://www.ncbi.nlm.nih.gov/genome/1008. 2022.

622 [29] Moon K, Bonocora RP, Kim DD, Chen Q, Wade JT, Stibitz S, et al. The BvgAS Regulon
623 of Bordetella pertussis. mBio 2017;8.
624 [30] de Gouw D, Serra DO, de Jonge MI, Hermans PW, Wessels HJ, Zomer A, et al. The
625 vaccine potential of Bordetella pertussis biofilm-derived membrane proteins. Emerg Microbes
626 Infect 2014;3:e58.
627 [31] Carriquiriborde F, Martin Aispuro P, Ambrosis N, Zurita E, Bottero D, Gaillard ME, et al.
628 Pertussis Vaccine Candidate Based on Outer Membrane Vesicles Derived From Biofilm
629 Culture. Front Immunol 2021;12:730434.
630 [32] Szklarczyk D, Kirsch R, Koutrouli M, Nastou K, Mehryary F, Hachilif R, et al. The
631 STRING database in 2023: protein-protein association networks and functional enrichment
632 analyses for any sequenced genome of interest. Nucleic Acids Res 2023;51:D638-d46.
633 [33] Ashniev GA, Sernova NV, Shevkoplias AE, Rodionov ID, Rodionova IA, Vitreschak AG,
634 et al. Evolution of transcriptional regulation of histidine metabolism in Gram-positive bacteria.
635 BMC Genomics 2022;23:558.
636 [34] Kurushima J, Kuwae A, Abe A. Iron starvation regulates the type III secretion system in
637 Bordetella bronchiseptica. Microbiol Immunol 2012;56:356-62.
638 [35] Altindiş E, Tefon BE, Yildirim V, Ozcengiz E, Becher D, Hecker M, et al.
639 Immunoproteomic analysis of Bordetella pertussis and identification of new immunogenic
640 proteins. Vaccine 2009;27:542-8.
641 [36] Tefon BE, Maass S, Ozcengiz E, Becher D, Hecker M, Ozcengiz G. A comprehensive
642 analysis of Bordetella pertussis surface proteome and identification of new immunogenic
643 proteins. Vaccine 2011;29:3583-95.
644 [37] Luu LDW, Octavia S, Zhong L, Raftery MJ, Sintchenko V, Lan R. Proteomic Adaptation
645 of Australian Epidemic Bordetella pertussis. Proteomics 2018;18:e1700237.

646 [38] Luu LDW, Octavia S, Zhong L, Raftery MJ, Sintchenko V, Lan R. Comparison of the
647 Whole Cell Proteome and Secretome of Epidemic Bordetella pertussis Strains From the 2008-
648 2012 Australian Epidemic Under Sulfate-Modulating Conditions. Front Microbiol
649 2018;9:2851.
650 [39] Midha MK, Kusebauch U, Shteynberg D, Kapil C, Bader SL, Reddy PJ, et al. A
651 comprehensive spectral assay library to quantify the Escherichia coli proteome by
652 DIA/SWATH-MS. Sci Data 2020;7:389.
653 [40] Kroes MM, Miranda-Bedate A, Hovingh ES, Jacobi R, Schot C, Pupo E, et al. Naturally
654 circulating pertactin-deficient Bordetella pertussis strains induce distinct gene expression and
655 inflammatory signatures in human dendritic cells. Emerg Microbes Infect 2021;10:1358-68.
656 [41] Dienstbier A, Amman F, Petráčková D, Štipl D, Čapek J, Zavadilová J, et al. Comparative
657 Omics Analysis of Historic and Recent Isolates of Bordetella pertussis and Effects of Genome
658 Rearrangements on Evolution. Emerg Infect Dis 2021;27:57-68.
659 [42] Lv Z, Yin S, Jiang K, Wang W, Luan Y, Wu S, et al. The whole-cell proteome shows the
660 characteristics of macrolides-resistant Bordetella pertussis in China linked to the biofilm
661 formation. Arch Microbiol 2023;205:219.
662 [43] Ashworth LA, Irons LI, Dowsett AB. Antigenic relationship between serotype-specific
663 agglutinogen and fimbriae of Bordetella pertussis. Infect Immun 1982;37:1278-81.
664 [44] Wang H, Wilksch JJ, Chen L, Tan JW, Strugnell RA, Gee ML. Influence of Fimbriae on
665 Bacterial Adhesion and Viscoelasticity and Correlations of the Two Properties with Biofilm
666 Formation. Langmuir 2017;33:100-6.
667 [45] Hiramatsu Y, Saito M, Otsuka N, Suzuki E, Watanabe M, Shibayama K, et al. BipA Is
668 Associated with Preventing Autoagglutination and Promoting Biofilm Formation in Bordetella
669 holmesii. PLoS One 2016;11:e0159999.

[46] Menozzi FD, Boucher PE, Riveau G, Gantiez C, Locht C. Surface-associated filamentous hemagglutinin induces autoagglutination of Bordetella pertussis. Infect Immun 1994;62:4261-9.

[47] Scheller EV, Cotter PA. Bordetella filamentous hemagglutinin and fimbriae: critical adhesins with unrealized vaccine potential. Pathog Dis 2015;73:ftv079.

[48] Hazenbos WL, van den Berg BM, Geuijen CW, Mooi FR, van Furth R. Binding of FimD on Bordetella pertussis to very late antigen-5 on monocytes activates complement receptor type 3 via protein tyrosine kinases. J Immunol 1995;155:3972-8.

[49] Barkoff AM, Mertsola J, Pierard D, Dalby T, Hoegh SV, Guillot S, et al. Surveillance of Circulating Bordetella pertussis Strains in Europe during 1998 to 2015. J Clin Microbiol 2018;56.

[50] Mir-Cros A, Moreno-Mingorance A, Martín-Gómez MT, Abad R, Bloise I, Campins M, et al. Pertactin-Deficient Bordetella pertussis with Unusual Mechanism of Pertactin Disruption, Spain, 1986-2018. Emerg Infect Dis 2022;28:967-76.

[51] Kastrin T, Barkoff AM, Paragi M, Vitek MG, Mertsola J, He Q. High prevalence of currently circulating Bordetella pertussis isolates not producing vaccine antigen pertactin in Slovenia. Clin Microbiol Infect 2019;25:258-60.

[52] Carbonetti NH. Pertussis toxin and adenylate cyclase toxin: key virulence factors of Bordetella pertussis and cell biology tools. Future Microbiol 2010;5:455-69.

[53] Mooi FR, van Loo IH, van Gent M, He Q, Bart MJ, Heuvelman KJ, et al. Bordetella pertussis strains with increased toxin production associated with pertussis resurgence. Emerg Infect Dis 2009;15:1206-13.

[54] Kollmann TR, Levy O, Montgomery RR, Goriely S. Innate immune function by Toll-like receptors: distinct responses in newborns and the elderly. Immunity 2012;37:771-83.

694 [55] Chow MY, Khandaker G, McIntyre P. Global Childhood Deaths From Pertussis: A
695 Historical Review. Clin Infect Dis 2016;63:S134-s41.
696 [56] Luzina IG, Keegan AD, Heller NM, Rook GA, Shea-Donohue T, Atamas SP. Regulation
697 of inflammation by interleukin-4: a review of "alternatives". J Leukoc Biol 2012;92:753-64.
698 [57] Baggiolini M, Clark-Lewis I. Interleukin-8, a chemotactic and inflammatory cytokine.
699 FEBS Lett 1992;307:97-101.
700 [58] Lopez-Castejon G, Brough D. Understanding the mechanism of IL-1β secretion. Cytokine
701 Growth Factor Rev 2011;22:189-95.
702 [59] Boyman O, Sprent J. The role of interleukin-2 during homeostasis and activation of the
703 immune system. Nat Rev Immunol 2012;12:180-90.
704 [60] Tanaka T, Narazaki M, Kishimoto T. IL-6 in inflammation, immunity, and disease. Cold
705 Spring Harb Perspect Biol 2014;6:a016295.
706 [61] Ausiello CM, Mascart F, Corbière V, Fedele G. Human Immune Responses to Pertussis
707 Vaccines. Adv Exp Med Biol 2019;1183:99-113.
708 [62] Warfel JM, Zimmerman LI, Merkel TJ. Acellular pertussis vaccines protect against disease
709 but fail to prevent infection and transmission in a nonhuman primate model. Proc Natl Acad
710 Sci U S A 2014;111:787-92.
711 [63] Alexander F, Matheson M, Fry NK, Labram B, Gorringe AR. Antibody responses to
712 individual Bordetella pertussis fimbrial antigen Fim2 or Fim3 following immunization with the
713 five-component acellular pertussis vaccine or to pertussis disease. Clin Vaccine Immunol
714 2012;19:1776-83.
715 [64] Hallander H, Advani A, Alexander F, Gustafsson L, Ljungman M, Pratt C, et al. Antibody
716 responses to Bordetella pertussis Fim2 or Fim3 following immunization with a whole-cell, two-
717 component, or five-component acellular pertussis vaccine and following pertussis disease in
718 children in Sweden in 1997 and 2007. Clin Vaccine Immunol 2014;21:165-73.

719 [65] Kroes MM, Miranda-Bedate A, Jacobi RHJ, van Woudenbergh E, den Hartog G, van
720 Putten JPM, et al. Bordetella pertussis-infected innate immune cells drive the anti-pertussis
721 response of human airway epithelium. Sci Rep 2022;12:3622.
722 [66] Pederick VG, Eijkelkamp BA, Ween MP, Begg SL, Paton JC, McDevitt CA. Acquisition
723 and role of molybdate in Pseudomonas aeruginosa. Appl Environ Microbiol 2014;80:6843-52.
724 [67] Zhang Y, Gladyshev VN. Molybdoproteomes and evolution of molybdenum utilization. J
725 Mol Biol 2008;379:881-99.
726 [68] Vidakovics ML, Paba J, Lamberti Y, Ricart CA, de Sousa MV, Rodriguez ME. Profiling
727 the Bordetella pertussis proteome during iron starvation. J Proteome Res 2007;6:2518-28.
728
729

Figure Legends

Fig. 1: **Abundance of 4 proteins involved in virulence by FIM2 and FIM3 isolates based on PRM absolute quantification**
Cellular abundance of 4 different virulence factors: **(A) S1-PT, (B) PRN, (C) FHA, (D) FIM and (E) AC-Hly**, were measured by PRM [in grams (g)] in 8 FIM2 isolates (FR5510, FR5810, FR5862, FR5994, FR6156, FR6440, FR6762, FR6845, blue dot) and 6 FIM3 isolates (FR4887, FR5031, FR5333, FR5782, FR5893, FR6167, black dot). Each dot represents the mean protein amount of 5 independent experiments. Levels of measured proteins are represented in median and interquartile. P-value <0.05 of the Mann-Whitney test between FIM2 and FIM3 serotype group was considered significant.

Fig. 2: Auto-agglutination, biofilm formation and survival in blood of FIM2 and FIM3 isolates
Biological phenotypes of 8 FIM2 isolates (FR5510, FR5810, FR5862, FR5994, FR6156, FR6440, FR6762, FR6845, blue dot), 6 FIM3 isolates (FR4887, FR5031, FR5333, FR5782, FR5893, FR6167 black dot), were compared in terms of: **(A) Auto-agglutination** property based on an auto-agglutination index ($OD_{650\ nm}$ at H0- $OD_{650\ nm}$ at H4)*100, **(B) Biofilm formation after 24 hours** and **(C) 48 hours of incubation** (Crystal Violet 0.1% $OD_{595\ nm}$). The 3 FIM- isolates (FR4922, FR4925, FR5167, orange dot) and one isolate that do not produce FHA (CIP1672, Ctrl, grey dot) were used as controls. **(D) Bacterial survival rate** (%) after 4 hours in whole cord blood (MOI=10) was quantified in CFU/ml for a subset of 2 different FIM2 (FR5862, FR6440, in blue) and 2 FIM3 (FR4887, FR5333, in black) isolates. Each dot represents the mean of 3 independent experiments for each isolate. Measures of IIA, Biofilm and survival are represented in median and interquartile. P<0.05 of the Kruskall Wallis followed by Dunn's comparison for auto-agglutination and biofilm and Mann Whitney test between FIM2 and FIM3 for survival, was considered significant.

Fig. 3: Cytokine release after infection of whole cord blood cells by FIM2 and FIM3 isolates
Cord blood [28] from healthy donors (n=9) was infected ex vivo with FIM2 isolates (FR5862 and FR6440, expected MOI of 10, 6.55 x 10^7 to 1.84 x 10^8 CFU/ml) or FIM3 isolates (FR5333, expected MOI of 10, 7.7 x 10^7 to 3.5 x 10^8 CFU/ml). Analytes were measured in whole blood supernatants after 22 hours of infection using a panel of 19 cytokines/chemokines (Human Magnetic Luminex Assay 20 Plex kit) **(A)** The heatmap represents a hierarchical clustering of all the cytokines, chemokines and growth factors differentially secreted (adjusted p-value<0.05) upon stimulation with FIM2 isolates (in blue) and by FIM3 isolates (in black). Cytokines are expressed as pg/ml and log transformed with blue to red colors representing lower to higher expression respectively. Levels (in pg/ml) of **(B)** IL-4, **(C)** IL-8, **(D)** IL-2 and **(E)** IL-6 in whole cord blood following infection with FIM2 (in blue) and FIM3 (in black) isolates are represented in median and interquartile. Each dot represents an experiment. P-value <0.05 of the Mann-Whitney test between FIM2 and FIM3 serotype group was considered significant.

Fig. 4: Abundance of 4 proteins involved in virulence by FIM3 isolates from clade 1 and 2 based on PRM absolute quantification
Cellular abundance of 4 different virulence factors: **(A) FIM3, (B) S1-PT, (C) PRN, (D) AC-Hly, (E) FHA**, were measured by PRM [in grams (g)] in 6 FIM3 isolates from clade 1 (FR4887, FR5031, FR5333, FR5782, FR5893, FR6167) and 5 isolates from clade 2 (FR3977, FR4930, FR5468, FR5730, FR5771). Each dot represents the mean of 5 independent experiments for each isolate. Levels of measured proteins are represented in median and interquartile. P-value <0.05 of the Mann-Whitney test between FIM2 and FIM3 serotype group was considered significant.

Fig. 5: Auto-agglutination, biofilm formation and survival in blood of *B. pertussis* isolates from clade 1 and 2.
Biological phenotypes of 6 FIM3 isolates from clade 1 (FR4887, FR5031, FR5333, FR5782, FR5893, FR6167, black dot) and 5 FIM3 isolates from clade 2 (FR3977, FR4930, FR5468, FR5730, FR5771, green dot) were compared in terms of: **(A) Auto-agglutination** property based on an auto-agglutination index (OD650nm at H0 – OD650 nm at H4)*100, **(B) Biofilm formation at 24 hours** and **(C) 48 h of incubation** (Crystal Violet 0.1% OD595nm). One isolate that do not produce FHA (CIP1672, Ctrl, grey dot) was used as control. **(D) Bacterial survival rate** (%) after 4 h in whole cord blood (MOI=10) was quantified in CFU/ml for a subset of 2 FIM3 isolates from clade 1 (FR4887, FR5333, in black) and 2 FIM3 isolates from clade 2 (FR4930, FR5730, in green) and expressed in %. Each dot represents the the mean of 3 independent experiments for each isolate. Levels of each measure are represented in median and interquartile. P<0.05 of the Kruskall Wallis followed by Dunn's comparison test for auto-agglutination, and Mann Whitney test between clade 1 and clade2 for biofilm and survival, was considered significant.

Fig. 6: Large-scale proteomic analysis according to FIM serotype
8 FIM2 isolates (FR5510, FR5810, FR5862, FR5994, FR6156, FR6440, FR6762, FR6845) and 6 FIM3 isolates (FR4887, FR5031, FR5333, FR5782, FR5893, FR6167) were used for the DIA-MS acquisition. Our pre-defined selection criteria were a |log2(FC)|>1 with an adjusted p-value<0.01 and a FDR<1%). **(A)Volcano plot** showing the differential proteins between FIM2 and FIM3 isolates. Each dot represents the mean protein amount of 3 independent replicates. The red dots represent proteins that are significantly more abundant and the blue dots proteins that are significantly less abundant in FIM2 compared to FIM3 isolates. **(B) Heatmap** display the mean z-scores of proteins with small p-values (p-value<1 %) along FIM2 and FIM3 isolates. Hierarchical clustering on the left side of the heatmap is estimated from the mean z-scores using a Pearson correlation-based distance and the Ward's method.

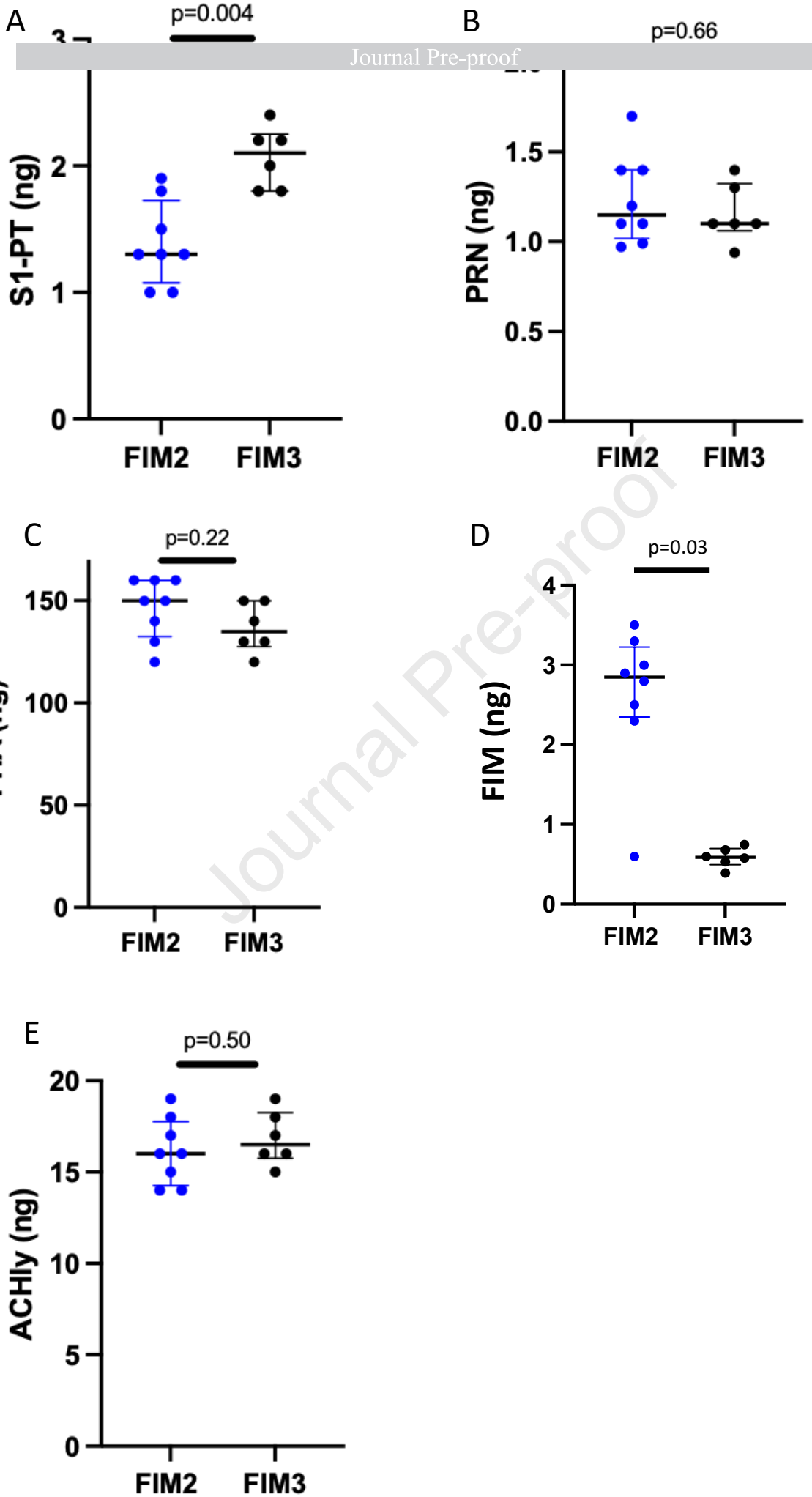

A-Auto-Agglutination

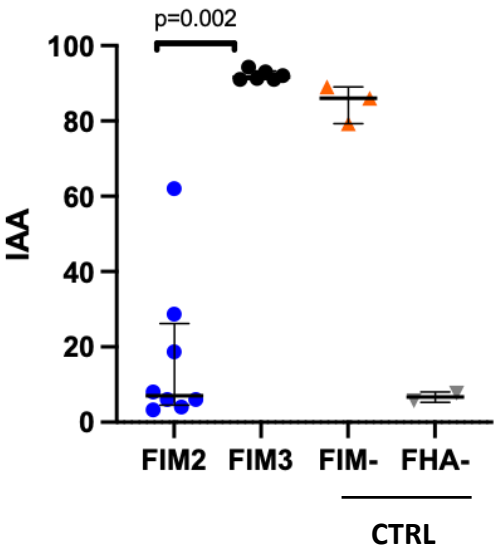

B-Biofilm H24

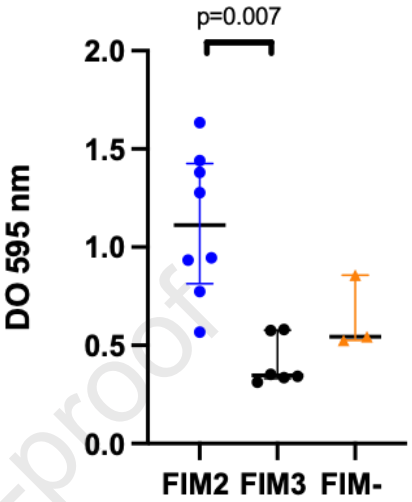

C-Biofilm H48

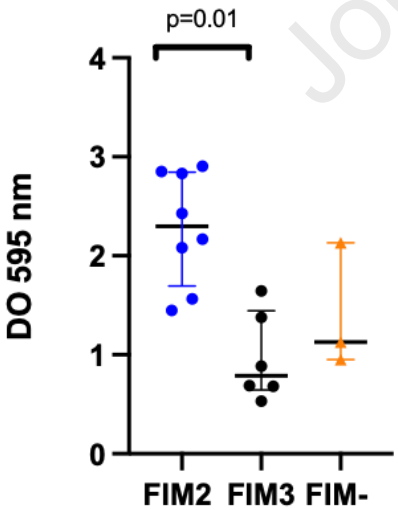

D-Survival rate

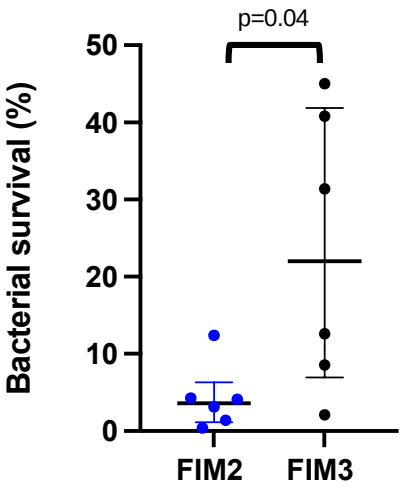

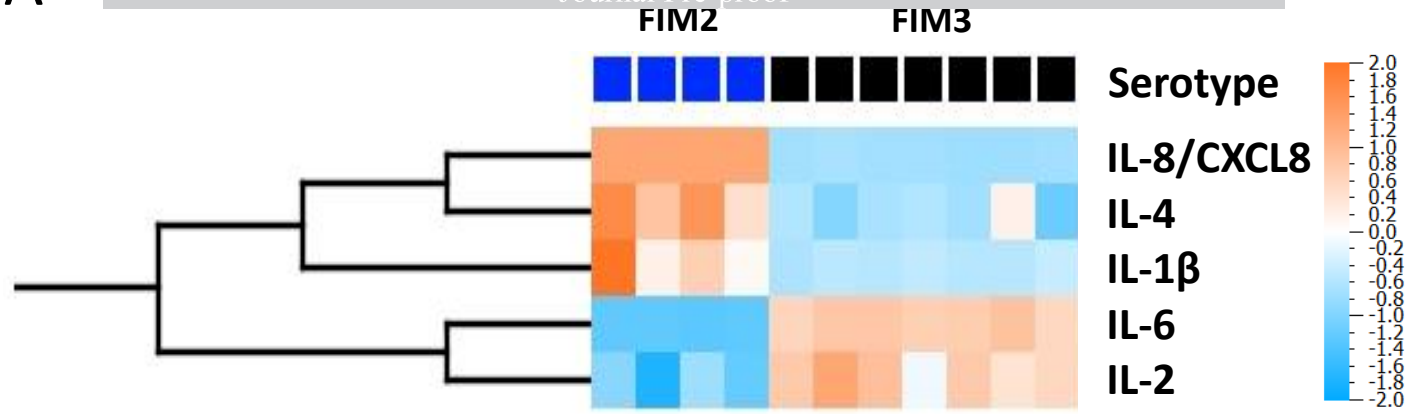

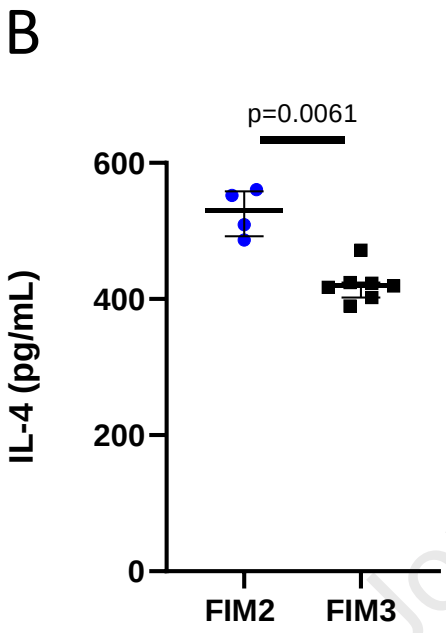

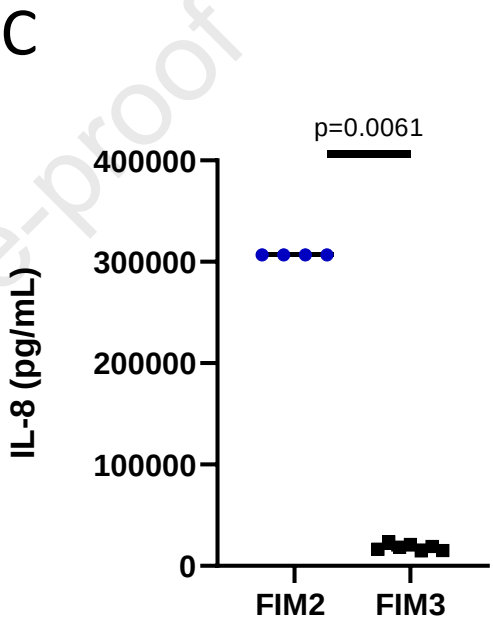

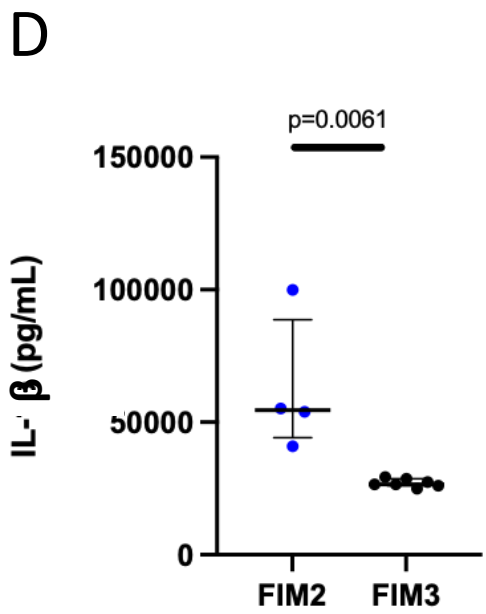

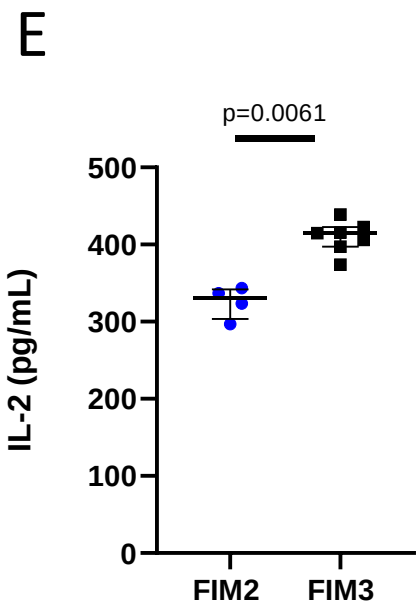

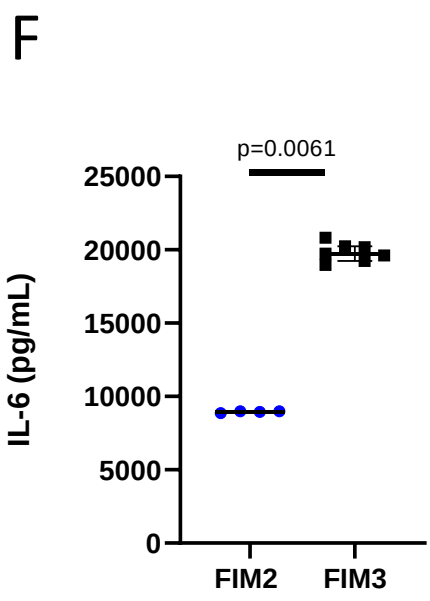

A

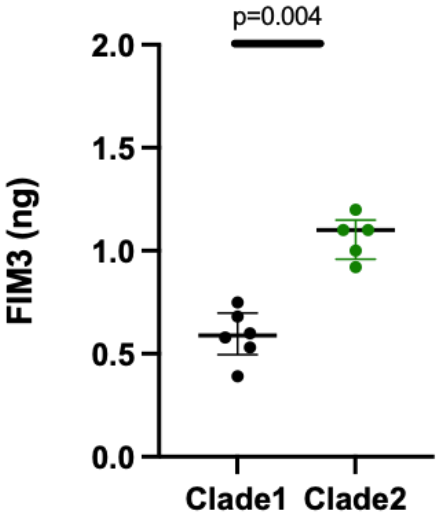

B

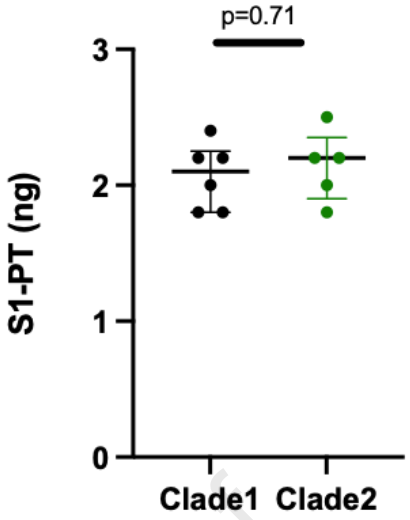

C

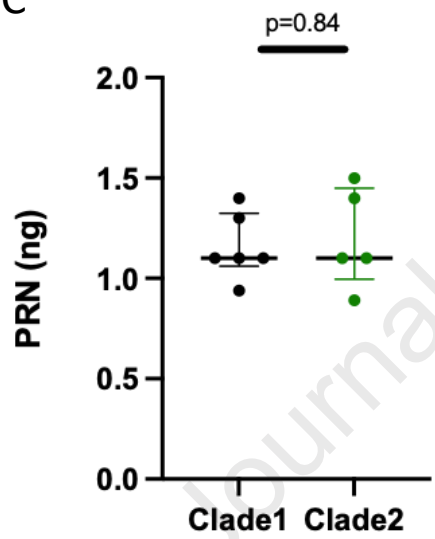

D

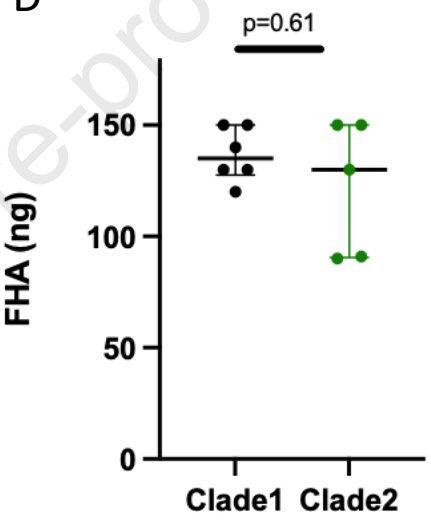

E

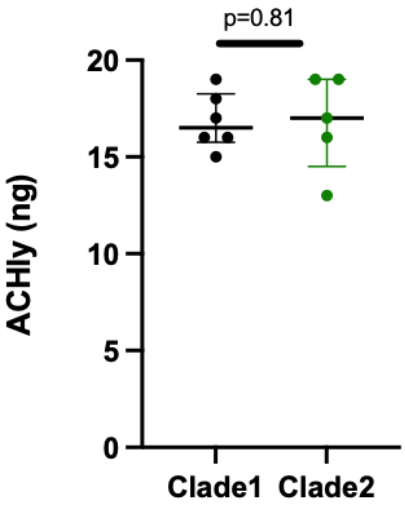

A-Auto-Agglutination

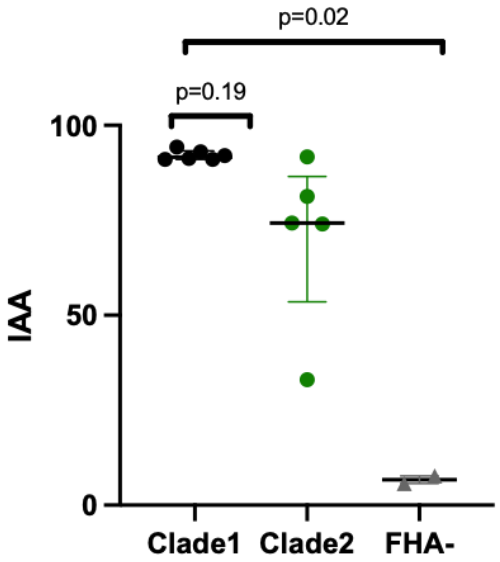

B-Biofilm H24

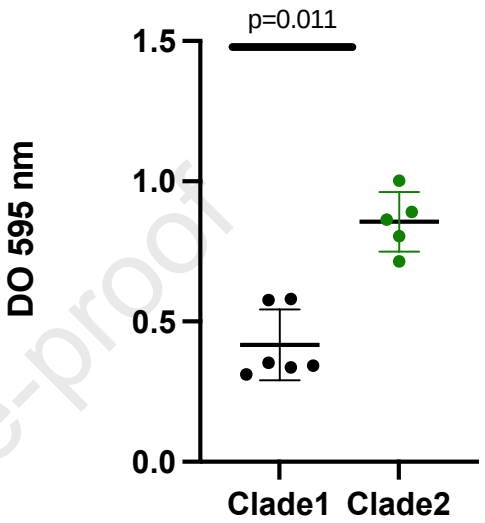

C-Biofilm H48

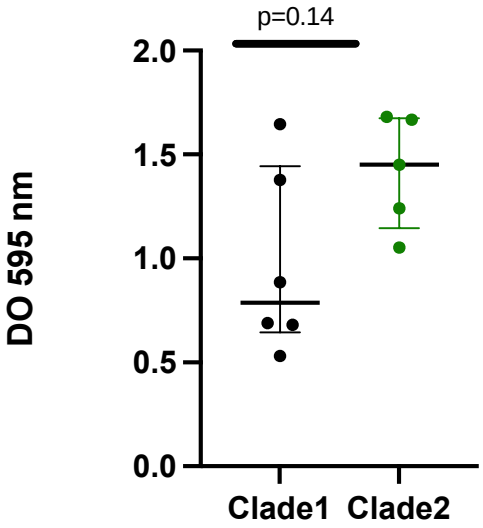

D-Survival rate

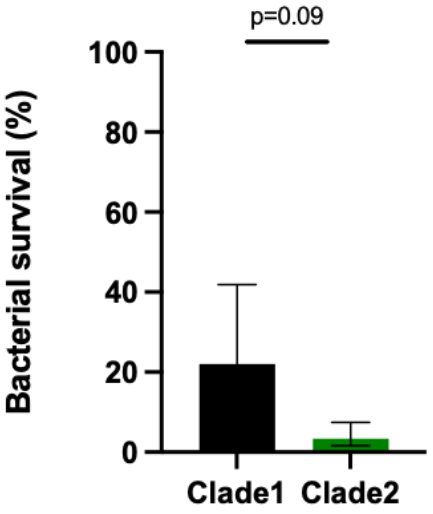

A

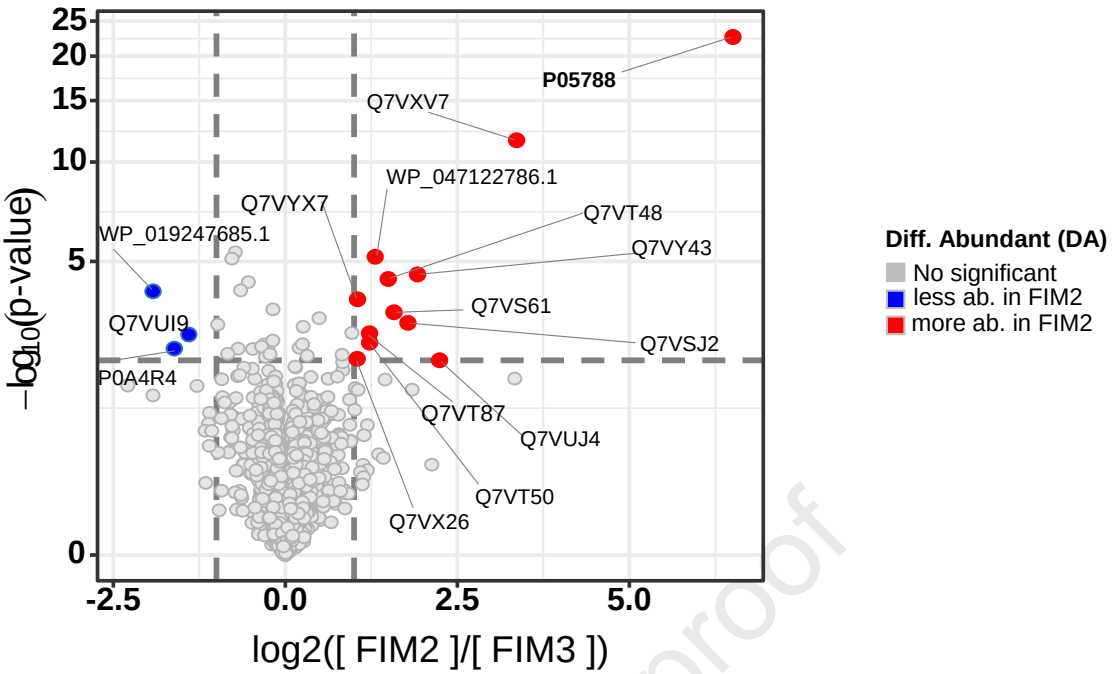

B